

# Long-range superior mirages

Waldemar H. Lehn and Thomas L. Legal

Superior mirages of simple appearance are occasionally observed over distances exceeding 70 km. These mirages cannot be explained in terms of standard textbook models; rather, they are shown to arise from fairly complex atmospheres. Two observations of different types, observed at Resolute Bay, Canada, are presented. The first is the basic three-image mirage in which one inverted and one erect image float above the object. The second is a single-image mirage in which the object is elevated but undistorted. For each, the most suitable atmospheric model contains several distinct atmospheres, and the first one requires sloped atmospheric layers as well. © 1998 Optical Society of America

*OCIS codes:* 010.1290, 010.3920, 010.4030.

## 1. Introduction

We have observed numerous superior mirages at great distances, ranging from 70 to 105 km. There exists an interesting paradox in the nature of such mirages. Complex mirages can often be explained in terms of a simple atmospheric model: an ordinary widespread temperature inversion that produces an optical duct.<sup>1,2</sup> To explain mirages of simple appearance, on the other hand, it is shown that relatively complex models are required. Such mirages do not look significantly different from short-range mirages, but it appears that, to our knowledge, no one has published an analysis that identifies the appropriate atmospheric conditions.

Two observations are analyzed here. Both were photographed from the Polar Continental Shelf Project camp at Resolute Bay, Northwest Territories, Canada, in 1994. Both are of simple appearance and were observed over a very long range. The first contains an inverted and an erect image elevated above the object, and the second is an even simpler lifting into view of a distant peak. They are discussed separately in the sections below. Several competing models are presented for each, and the most physically reasonable one is selected and described.

The standard textbook model for the first case<sup>3–5</sup> is the elevated temperature inversion. It contains a rapid drop of the refractive index with increasing height, which causes rays to be refracted downward. Rays leaving the object with an upward heading are refracted down to enter the observer's eye. Because the refraction is localized within a narrow band of elevations, the ray paths behave almost as if reflected from an elevated mirror. These rays produce an elevated inverted image of the object, usually topped by a compressed erect image. This model works well for mirages for which the viewing range is short to moderate—say of the order of 25 km or less. It does not, however, work for longer ranges, mainly because of the increased effects of the Earth's curvature in these cases.

For the second type, the observer is typically placed within an atmosphere whose temperature rises uniformly with elevation.<sup>6–8</sup> Light rays are all refracted downward, but this time the rays do not cross each other as in the above case. The visual effect is to lift distant objects but not to distort them. Again for very long ranges the case is not quite so simple.

## 2. Somerset Mirage

### A. Observation

This mirage is an image of two peaks on Somerset Island as seen from Resolute Bay at 07:35 Central Daylight Time (CDT) on 4 June 1994. The line of sight is nearly due south. The onset of the mirage was not observed, but we estimate that it lasted largely unchanged for approximately half an hour. The mirage and its corresponding undistorted image are shown in Fig. 1. The highest peak in the image has an elevation of 340 m above sea level, and its

W. H. Lehn is with the Department of Electrical and Computer Engineering, University of Manitoba, Winnipeg R3T 5V6, Canada. T. L. Legal is with MPR Teltech, Ltd., 8999 Nelson Way, Burnaby, British Columbia V5A 4B5, Canada.

Received 24 June 1997; revised manuscript received 2 September 1997.

0003-6935/98/091489-06\$15.00/0  
© 1998 Optical Society of America

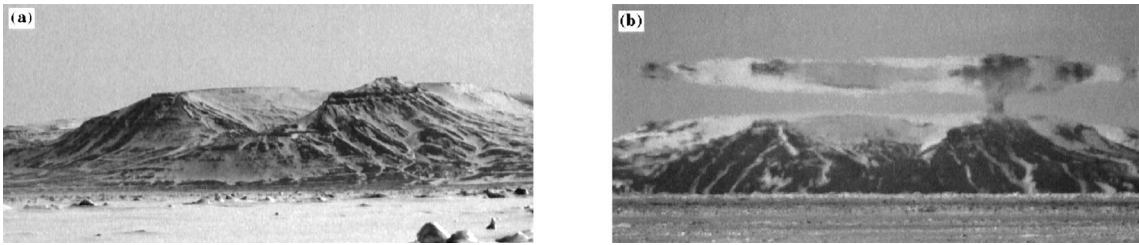


Fig. 1. (a) Normal view of the Somerset peaks from a distance of 19 km, (b) superior mirage from 77.7 km. The peaks look smaller in (b) because the intervening ice horizon cuts off the lower portion of the image.

distance from the camera (elevation 67 m) is 77.7 km. The observational geometry in geographic profile is shown in Fig. 2; here the Earth is represented as flat, so that straight rays appear to curve upward. As measured by theodolite, the image spans 17.4 arc min vertically: the horizon is at  $-13.3$  arc min and the top of the mirage is at  $4.1$  arc min. During the whole observation, no short-range (less than 25-km) mirages were seen, nor did any long-range (75-km) mirages exist to the west. The map of Fig. 3 shows the relation to local land masses.<sup>9</sup>

At the time of the mirage, the barometer was steady at 101.04 kPa and the temperature was  $1.5^{\circ}\text{C}$  (data from the surface weather record, Resolute). A local temperature profile measured by the Atmospheric Environment Service (AES) at 07:00 hours CDT was also available (Fig. 4, curve 4). The surface wind was slowly rising and shifting: at 07:00,

12 kn at  $120^{\circ}$ ; at 08:00, 18 kn at  $130^{\circ}$ ; by noon settled in  $\sim 12$  kn at  $150^{\circ}$ .

## B. Model 1

The simplest model for any mirage simulation, the single spherically symmetric atmosphere concentric with the Earth, will be applied first. In considering the ray paths required for producing the observation, we will use the traditional convention of reversing ray directions and think of a ray bundle that emanates from the observer's eye.

The lower part of the image in Fig. 1(b) is undistorted, and the measured elevation of the ice horizon ( $-13.3$  arc min) is the value expected in a standard atmosphere. It follows that the rays producing this part of the image undergo minimal refraction and propagate in almost straight lines. This implies a relatively nominal atmosphere for the air layers from the surface up to the peak elevation of 340 m (the zone between rays 1 and 2 in Fig. 2). The rays within this region leave the eye with very small elevation angles, but as they proceed on their very long paths, the Earth's curvature causes the local level reference to shift, and the rays cross the level layers at ever steeper angles. When they enter the inversion that produces the inverted image, which must exist at elevations above 340 m, their angles are so steep that enormous temperature gradients are required for turning them to a downward heading.

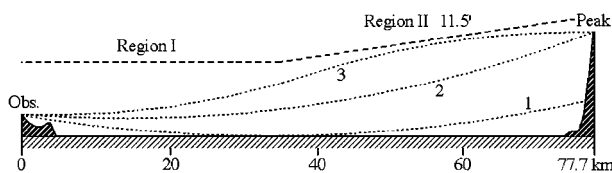


Fig. 2. Geographic profile with flattened Earth and magnified vertical scale. Regions I and II apply to the third model for the Somerset mirage.

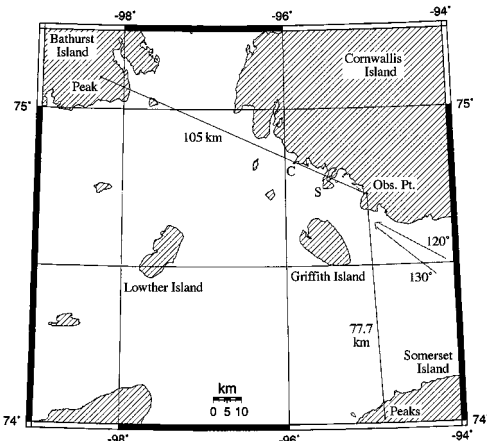


Fig. 3. Map of the Resolute region. The letters C and S on the line of sight to Bathurst Island identify Claxton Point and Sheringham Point, respectively.

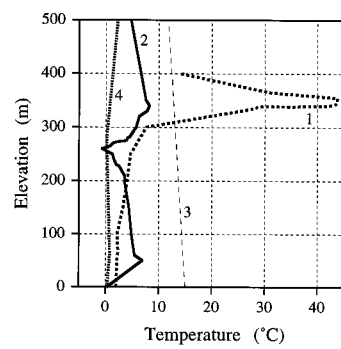


Fig. 4. Temperature profiles. Curves 1 and 2 represent models 1 and 2 of the Somerset mirage. The curve for model 2, the sloped atmosphere, represents the profile at the distance of 77.7 km from the observer. Straight line 3, which has a lapse rate of  $6.5^{\circ}/\text{km}$ , gives the standard atmosphere<sup>10</sup> for comparison. Curve 4 is the profile measured by the AES.

The mirage can be successfully simulated,<sup>11</sup> but the atmosphere is completely unrealistic, with an inversion strength of over 40 °C (see temperature profile 1 of Fig. 4). This result is basically the same whether or not we use the AES profile as a basis.

Model 1 fails to handle this case well because of two factors: the large elevation difference between observer and target and the significant curvature of the Earth over the range.

### C. Model 2

A second model that can be considered is the single sloped atmosphere. Perner and Exner<sup>12</sup> considered this model of practical importance, but did not proceed to study it. It is basically the spherical shell model in which the shells are concentric with each other but not with the Earth. The slope is adjusted so that the elevation of the inversion above the observer's head is roughly the same as its elevation above the peaks. This model solves the problem of extreme temperature variation. An exploration of parameter space produces a good image simulation with a layer slope of 11.5 arc min and a maximum temperature excursion of 9 °C. The temperature profile at 77.7 km is shown as curve 2 in Fig. 4. Because of its slope, the profile is 260 m lower at the observer's location. The model is again physically unrealistic: aside from demanding a uniform slope of the air layers over ~65 km of sea ice, it requires extremely unstable temperature gradients.

### D. Model 3

The third model, which we propose as the most reasonable for this observation, exhibits the minimum extremes in atmospheric conditions. The same model arises in the analysis of Lowther Island mirages, reported in Ref. 13. It consists of a two-stage atmosphere: level layers in the observer's region and sloped layers in the area near the peaks. Although the transition between the regions is unrealistically abrupt, the insertion of a third intermediate atmosphere to smooth the change does not significantly alter the images or the original two atmospheres. Considering the wind at the time of observation (between 12 and 18 kn, at 120° to 130°; see map, Fig. 3), it might be reasonable to expect air movement down and out over the sea from the uplands of Somerset Island, which are at ~350-m elevation. Figure 5(a) shows the two temperature profiles. The AES atmosphere is used for the near part (first 35 km; region I, Fig. 2), and the far atmosphere, region II, is constructed by a process of ray steering (by controlling ray vertices) to reproduce the mirage. The rays proceed roughly parallel to the air layers of region II so that a moderate inversion of 12 °C is enough to turn them downward [see Fig. 5(b)]. The simulated mirage is shown in Fig. 5(c), which should be compared with Fig. 1(b). The slope of the atmosphere, 11.5 arc min, is within the range considered reasonable for advection.<sup>14</sup> This model produces the least extreme atmosphere, in the sense

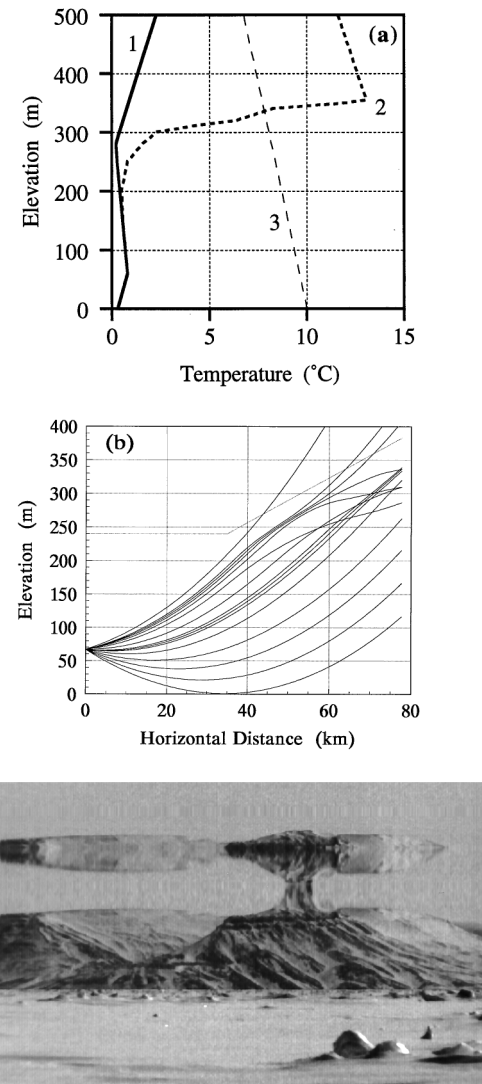


Fig. 5. (a) Temperature profiles for model 3: near atmosphere (solid curve 1), far atmosphere (dotted curve 2), standard atmosphere for comparison (dashed curve 3); (b) ray paths; (c) mirage simulation.

of limiting both inversion strength and horizontal extent, that is consistent with the observation.

A fourth model that does not require sloped atmospheres has been suggested by an unnamed reviewer. It is based on the following considerations. The mirage portion of the image is nearly centered on the astronomical horizon. The corresponding rays are therefore almost level in the vicinity of the observer. Such rays can easily be made to follow the paths required for creating the inverted image; all it takes is a small local inversion close to the observer. An example would be an inversion of 2° or 3° a few meters above the observer's head and extending from the observer out to ~10 km along the line of sight. Some experimental ray tracings show that mirage synthesis could be straightforward and quite exact. In the absence of other data this model would in fact be the best candidate by virtue of its simplicity. There are two factors that argue against the model in

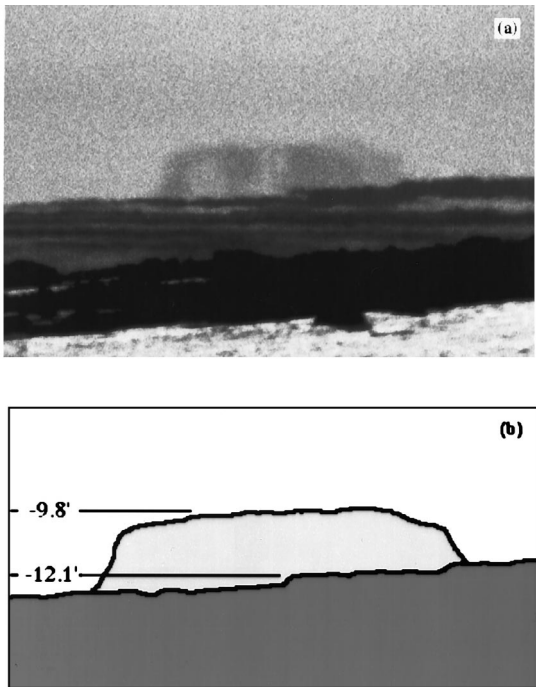


Fig. 6. (a) Bathurst Island mirage, (b) measured elevation angles of the mirage image.

the present case. A local inversion of this sort would produce a mirage of nearer objects such as Griffith Island, 25 km distant and  $28^\circ$  off the line of sight; such a mirage was not observed. Also the AES temperature profile measured 35 min earlier does not indicate a sufficient local inversion.

### 3. Bathurst Mirage

#### A. Observation

On 3 June 1994 at 19:36 CDT (00:36 UT, 4 June), an image of a peak on Bathurst Island suddenly appeared, where nothing was previously visible; it is the bump on the horizon in the center of Fig. 6(a). Theodolite readings simultaneous with the photograph give an image height of 2.3 arc min at the center and 2.8 arc min on the left-hand side of the mirage [see the outline drawing of Fig. 6(b)]. The peak has an elevation of 351 m. Its distance is 105 km from the camera, whose elevation is 67 m, as above. The mirage can be compared with a photograph taken from a 171-m hilltop at Resolute (Fig. 7), in which no mirage phenomena are evident. The mirage shows the top portion of the peak, largely undistorted. Some magnification is noticeable: The sides of the mirrored peak are somewhat steeper than those in the normal image. In the field the magnification was not obvious. This mirage is a case of looming,<sup>6</sup> in which a distant object is optically lifted into view while remaining recognizable and minimally distorted.

Meteorological conditions at the time of the observation were obtained from the surface weather record at Resolute. The pressure was 101.00 kPa and drop-

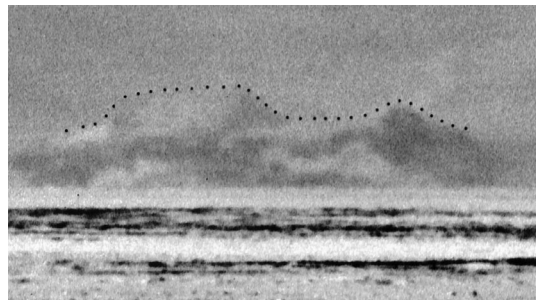


Fig. 7. Bathurst peak at a distance of 106 km, as seen from a hill of 171-m height at Resolute. To make the peak more visible, contrast has been enhanced and the peak has been outlined with dots.

ping, the temperature was  $2^\circ\text{C}$ , and the wind speed was 10 kn, bearing  $140^\circ$ . The time variation of these quantities is discussed below.

The geographic profile is more complex in this case (see Fig. 8). The line of sight passes over several islands and peninsulas, the more important being Sheringham Point at 16 km and Claxton Point at 28.5 km. In an atmosphere with a surface temperature of  $2^\circ\text{C}$  and a standard lapse rate of  $0.006^\circ/\text{m}$ , a ray leaving the observer at an elevation angle of  $-14.2$  arc min would be tangent to the sea surface at a distance of 32.4 km, just beyond Claxton Point. In this atmosphere the measured elevation angles of Claxton Point can be translated into elevations above sea level:  $-12.6$  and  $-12.1$  arc min become 14 and 18 m, respectively. A topographic map with a scale of 1:50,000 shows a fairly low elevation under the line of sight, a bit below the 50-ft (15.2-m) contour. This reasonably good agreement is the basis for assuming that the atmosphere is normal for the first 29 km, i.e., from the observer to Claxton Point. This assumption is used in both of the models below.

#### B. Model 1

A mild low-level temperature inversion beyond Claxton Point is sufficient to generate the observed mirage. We searched through a number of temperature pro-

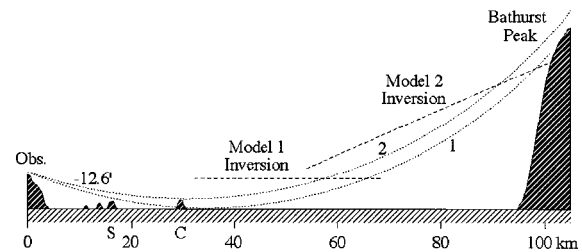


Fig. 8. Geographic profile for the Bathurst observation. Ray 1 is the horizon ray, with an elevation angle of  $-14.2$  arc min at the observer. This ray clears Sheringham Point (marked S) but is interrupted by Claxton Point (C). The lowest ray, 2, to clear Claxton Point has an elevation of  $-12.6$  arc min. In a standard atmosphere it passes well above the Bathurst peak. The dashed lines indicate the average height and the extent of the inversions used in models 1 and 2.

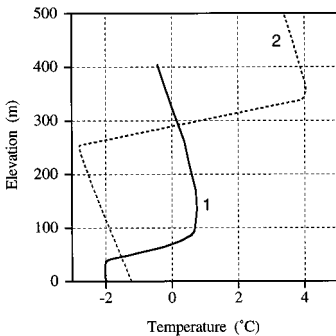


Fig. 9. Temperature profiles for the Bathurst mirage models. Curve 1 is the weak low-level inversion of model 1, lying just beyond Claxton Point. Curve 2 represents the sloping inversion of model 2 as it would appear at the Bathurst peak.

file shapes and elevations and various transition distances, again seeking the weakest inversion that could create the mirage.

The resulting profile is plotted in Fig. 9; this atmosphere is not sloped. Rays entering the inversion region are deflected downward a slight amount, so that the appropriate ones intersect the peak (see Fig. 10). Rays with elevation angles in the range from  $-12.6$  to  $-9.8$  arc min reach the top 37 m of the peak, in a uniformly distributed manner, producing a somewhat magnified ( $2.3 \times$  vertically) but otherwise undistorted image of the peak above Claxton Point, just like the observation. With such a simple ray distribution there is little point in displaying a mirage simulation.

The model calculations consider the second atmosphere to extend from 32 km all the way to Bathurst Island. In fact, the longitudinal extent of inversion could be much smaller, as all the rays have passed up through the inversion by the time they reach a distance of 68 km. A standard atmosphere used from 68 to 105 km produces the same rays.

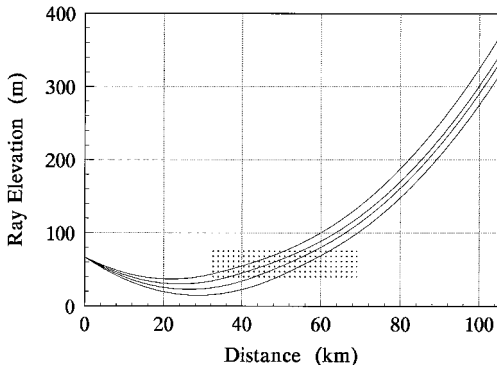


Fig. 10. Selected rays for model 1 of the Bathurst mirage. Ray elevation angles at the eye have the values of  $-12.5$  to  $-9.5$  arc min in 1-arc min intervals. The inversion, indicated by the dotted area, is centered on a 60-m elevation and extends from 32 to 68 km. In this region the flattening of the rays can be seen, as the inversion tries to straighten them.

### C. Model 2

Only one other model is analyzed here. It contains a standard atmosphere extending from the observer to 54 km, then an atmosphere with a slope of 15 arc min for the rest of the distance. Curve 2 of Fig. 9 shows the temperature profile of the second region as it would exist at 105 km. The ray paths are not plotted because they are similar to those of Fig. 10. The sloping inversion captures the upward-heading rays beyond Claxton Point and bends them downward sufficiently to intersect the peak, again with uniform spacing between successive rays. The rays with initial angles in the range from  $-12.6$  to  $-9.8$  arc min cover the top 89 m of the peak and produce an image that matches the observation, this time with unit magnification.

Both Bathurst models require only weak inversions. In this case we consider that the meteorological conditions favor model 1. The surface weather record shows relatively constant conditions during the three hours preceding 00:00 UT, but then several small abrupt changes occur between 00:00 and 01:00 UT, the hour that spans the observation time. The pressure drops from 101.03 to 100.99 kPa, and the temperature increases from 1.1 to 2.4 °C. The wind speed stays near 10 kn and its direction, although a bit erratic, tends from 170° to 130°. These conditions are consistent with a weak low-pressure region traveling toward the east. There is no doubt that the mirage is correlated with these events. The wind could have moved slightly warmed air from land to sea beyond Claxton Point if we allow a wind direction slightly more northerly than that observed at Resolute (see the map, Fig. 3). The warmer air flowing over and mixing with the cool surface air would create the necessary small inversion. On the other hand, there seems to be little physical reason for the sloping layers of model 2 to come into being.

### 4. Conclusions

Long-range superior mirages of the simplest appearance are caused by atmospheres of some complexity. The simple physical models that standard textbooks use to explain superior mirages and looming are not adequate. If unrealistically extreme atmospheric conditions are to be avoided, a successful model must include multiple-region atmospheres, sometimes incorporating sloping air layers.

The authors thank the Polar Continental Shelf Project, Natural Resources, Canada, for accommodation and logistic support at Resolute Bay; Nexus, Inc., Tokyo, Japan, for financial support; and Louis Legal, Atmospheric Environment Service, Winnipeg, Canada, for providing weather records.

### References and Notes

1. S. W. Visser, "The Novaya Zemlya phenomenon," Proc. K. Ned. Akad. Wet. Ser. B **59**, 375–385 (1956).
2. W. H. Lehn, "The Novaya Zemlya effect: an arctic mirage," J. Opt. Soc. Am. **69**, 776–781 (1979).
3. M. G. J. Minnaert, *Light and Color in the Outdoors* (Springer-Verlag, New York, 1993), p. 72.

4. W. J. Humphreys, *Physics of the Air*, 3rd ed. (Dover, New York, 1964), p. 472.
5. J. M. Pernter and F. Exner, *Meteorologische Optik*, 2nd ed. (Braumüller, Vienna, 1922), pp. 110ff, p. 125.
6. F. W. Sears, *Optics*, 3rd ed. (Addison-Wesley, Cambridge, Mass., 1949), p. 7 (looming).
7. Ref. 5, pp. 84ff (Erhebung).
8. Ref. 3, p. 61.
9. The map was obtained from a website entitled "Online Map Creation," at [www.aquarius.geomar.de](http://www.aquarius.geomar.de).
10. U.S. Standard Atmosphere, 1976, in R. G. Fleagle and J. A. Businger, *Introduction to Atmospheric Physics*, 2nd ed. (Academic, New York, 1980), p. 415.
11. W. H. Lehn and W. Friesen, "Simulation of mirages," *Appl. Opt.* **31**, 1267–1273 (1992).
12. Ref. 5, p. 109.
13. T. L. Legal, "Modelling of sloped atmosphere mirages," M.Sc. thesis (University of Manitoba, Winnipeg, Canada, 1995).
14. S. R. Church, "Atmospheric mirage and distortion modeling for IR target injection simulations," in *Targets and Backgrounds: Characterization and Representation II*, W. R. Watkins and D. Clement, eds., Proc. SPIE **2742**, 122–135 (1996).